Comparison of the Scope of True and Integrated Bipolar Leads in Implantable Cardioverter Defibrillators

J Requena-Carrión[1], J Väisänen[2], F Alonso-Atienza[1],
JL Rojo-Álvarez[1], J Hyttinen[2], A García-Alberola[3]

[1]Universidad Rey Juan Carlos, Fuenlabrada, Spain
[2]Ragnar Granit Institute, Tampere, Finland
[3]Hospital Universitario Virgen de la Arrixaca, Murcia, Spain

Abstract

Lead design is a critical factor for detecting and redetecting lethal arrhythmias in electrograms (EGM) from Implantable Cardioverter Defibrillators (ICD). The estimation of the scope of a lead can help to elucidate the anatomical origin of recorded EGM and explain signal features. In this paper, we compare quantitatively the scope of true and integrated bipolar sensing leads by combining bioelectric signal modeling and numerical analysis. We define the scope in terms of the Mean Square Difference (MSD) between the EGM generated by the whole ventricular myocardium and the EGM generated by smaller regions within the ventricular myocardium. Results show that integrated bipolar leads have a wider scope than true bipolar leads, although narrower than unipolar leads. Further, the extent of myocardium within the scope is distributed for integrated bipolar leads along the septum and anteriorly, while for true bipolar leads is located close to the electrode site.

1. Introduction

The Implantable Cardioverter Defibrillator (ICD) is nowadays the primary treatment for patients at high risk of Sudden Cardiac Death (SCD). Detection of lethal arrhythmias and redetection after a failed shock involve both appropriate detection algorithms and reliable sensing of electrograms (EGM) by transvenous lead systems. An excellent review of detection algorithms in ICD can be found in [1]. Current transvenous lead systems can incorporate two types of rate-sensing: true bipolar and integrated bipolar [2]. True bipolar leads consist of a tip and a ring electrodes, whereas integrated bipolar leads consist of a tip electrode and a distal coil (Figure 1). The design of sensing leads is a critical factor in the detection performance of the ICD and can affect EGM features such as the duration of complexes [3], recording of artifacts [4] and sensing latency [5] [6]. Discrepancies in the sensing performance of leads are often ascribed to differences in the scope. The scope of leads has been assessed based in the principles of Lead Field analysis introduced by McFee and Johnston [7]. According to Lead Field Theory, in an infinite and homogeneous medium the scope is global for unipolar leads and local for bipolar leads [8]. Nevertheless, the assessment of the scope still remains largely qualitatively and, to date, differences in the scope of true and integrated bipolar leads have not been determined.

In this paper we analyze quantitatively the scope of true and integrated bipolar sensing leads. We define the scope in terms of the Mean Square Difference (MSD) between the EGM signal induced by the whole myocardium and the EGM signal induced by smaller regions within the myocardium. By combining the measurement sensitivity distribution of a lead system calculated in a realistic 3D human thorax with a model of cardiac electrical activity, we simulate numerically EGM signals and calculate the MSD. We estimate the scope of true and integrated bipolar leads and, additionally, of a unipolar lead. We determine the myocardial mass within the scope of every lead and study its anatomical location and size.

2. Methods

2.1. Modeling EGM signals

Lead Field Theory constitutes a general framework to formulate signals recorded by lead systems [9]. Myocardial electric activity is modeled as a distribution of time-varying multiple dipoles, $\overline{J}_i[n]$, representing cardiac current sources. Lead properties are introduced through the concept of measurement sensitivity distribution, $\overline{J}_{LE}$, which describes the ability of the lead system to measure cardiac current sources throughout the myocardium. According to Lead Field Theory the relationship between cardiac signal $z[n]$ recorded at the leads and cardiac current

(a) (b)

Figure 1. Superior view of the ventricular myocardium as described by the VHM dataset. Right ventricle (RV) and left ventricle (LV) are, respectively, the regions below and above the dashed line. Panel (a) shows tip and $ring$ electrodes in RV corresponding to a true bipolar lead. Panel (b) shows tip and $coil$ electrodes in RV corresponding to an integrated bipolar lead. The unipolar lead was modeled as a tip electrode in RV and a can electrode in subpectoral position (not shown).

sources $\overline{J}_i[n]$ distributed throughout the myocardium V is:

$$z[n] = \sum_V \frac{1}{\sigma} \overline{J}_{LE} \cdot \overline{J}_i[n] \ , \tag{1}$$

where σ is the conductivity of the medium. Equation (1) provides, thus, a means of synthesizing cardiac signals from cardiac current sources.

We obtained the measurement sensitivity distribution by measuring in the conducting volume the gradient of the potential field generated when the electrodes are energized reciprocally with one unit of current. We described the conducting properties of the human body based on Finite Difference Methods (FDM) featuring the realistic 3D male thorax of the Visible Human Man dataset (VHM) [10]. In our model, 20 different tissue types were identified, and the whole volume was characterized by a resolution of $1.67mm \times 1.67mm \times 4mm$ in the heart and $1.67mm \times 1.67mm \times 8mm$ elsewhere. Ventricles comprised approximately 30000 nodes. Based on this model, we calculated the measurement sensitivity distribution for true bipolar, integrated bipolar and unipolar leads. The true bipolar lead was modeled as two point electrodes, tip and $ring$, located in the right ventricle (RV); integrated bipolar lead as a point electrode, tip, and a distal long electrode, $coil$, in RV; and unipolar lead as a point electrode in RV and a box electrode, can, in subpectoral position (Figure 1).

2.2. Numerical analysis of the scope of lead systems

The contribution to a cardiac signal of a myocardial region V_o such that $V_o \subseteq V$, where V is the whole myocardium, was quantified by determining the similarity in mean power between signals generated by V and by V_o. From (1), if V_c is the complementary myocardial region of V_o with respect to V, i.e., if V_o and V_c are two disjoint myocardial regions and $V = V_o \cup V_c$, signal $z[n]$ recorded by the lead system can be expressed as:

$$\begin{aligned} z[n] &= \sum_V \frac{1}{\sigma} \overline{J}_{LE} \cdot \overline{J}_i[n] = \\ &= \sum_{V_o} \frac{1}{\sigma} \overline{J}_{LE} \cdot \overline{J}_i[n] + \sum_{V_c} \frac{1}{\sigma} \overline{J}_{LE} \cdot \overline{J}_i[n] = \\ &= z_o[n] + z_c[n] \ , \end{aligned} \tag{2}$$

where $z_o[n]$ and $z_c[n]$ are the signals generated by V_o and V_c, respectively. The similarity between $z[n]$ and $z_o[n]$ was defined in terms of their Mean Square Difference (MSD):

$$\begin{aligned} MSD\{V_o\} &= E\left[(z[n] - z_o[n])^2\right] = \\ &= E\left[(z_c[n])^2\right] = \\ &= P_{z_c z_c} \ , \end{aligned} \tag{3}$$

where E denotes statistical mean. Thus, $MSD\{V_o\}$ is the error of approximating the signal $z[n]$ to $z_o[n]$. We divided $MSD\{V_o\}$ by the mean power of $z[n]$, $P_{zz} = E\left[(z[n])^2\right]$, in order to obtain a more convenient measure of similarity between $z[n]$ and $z_o[n]$ that is relative to the mean power of $z[n]$:

$$\begin{aligned} MSD_n\{V_o\} &= \frac{MSD\{V_o\}}{P_{zz}} = \\ &= \frac{P_{z_c z_c}}{P_{zz}} \ . \end{aligned} \tag{4}$$

We used (4) as a basis for investigating the scope of transvenous ICD lead systems in the ventricles. Fixing a level α, we defined the scope of a lead as the region of minimum size that involves an MSD_n smaller than α.

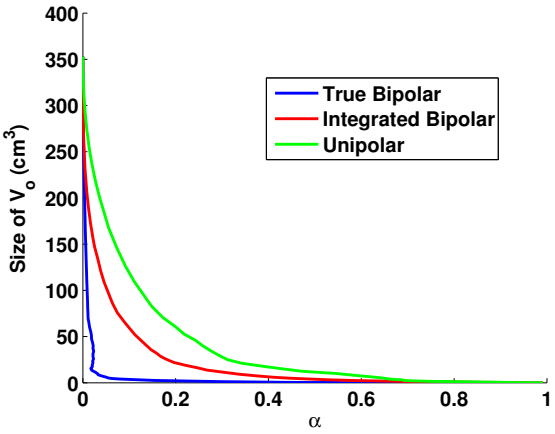

Figure 2. Size of the ventricular myocardium within the scope of implemented true and integrated bipolar and unipolar leads, versus α.

In order to estimate the contribution of a myocardial region V_o based on (4), a statistical description of cardiac current sources $\overline{J}_i[n]$ is needed. An alternative way is to generate cardiac current sources by means of computer simulations. We implemented a model of the electric activity of cardiac tissue previously defined [11] to numerically generate cardiac current sources. This model is based on the restitution properties of cardiac tissue, and is able to reproduce complex behavior, such as the restitution of Action Potential Duration (APD) and Conduction Velocity (CV), and curvature effects.

We simulated the stimulation of the apex at 60 beats per minute during 5 seconds. For every myocardial region V_o, simulated cardiac current sources were combined with the measurement sensitivity distribution according to (2) for synthesizing signals $z[n]$ and $z_o[n]$ for every lead configuration. Then, we replaced statistical means by time averages to estimate $MSD_n\{V_o\}$. We estimated the MSD_n for every member V_o of a family of myocardial regions consisting of the whole ventricular myocardium V, and progressively smaller nested myocardial regions, obtained by progressively eliminating the surfaces of lowest sensitivity. This choice of myocardial regions provides us with the regions of minimum size involving an MSD_n smaller than α [12].

3. Results

Computer simulations showed, as expected, that the size of the ventricular myocardium within the scope of a lead is a decreasing function of the parameter α (Figure 2). This observation can be explained by recalling that, according to (2), the larger V_o, the closer it is to V; consequently, the more similar z_o is to z and the smaller is $MSD_n\{V_o\}$.

The slope of the curves of the size of V_o against α reflects the rate of decrease of the measurement sensitivity of a lead system with the distance. The early slope was found to be steeper for bipolar than for unipolar leads. This observation agrees with the fact that, in an infinite and homogeneous medium, the measurement sensitivity distribution for unipolar leads decreases inversely to r^2, while for bipolar leads it decreases inversely to r^3, where r is the distance of cardiac current sources to the lead system [8]. Additionally, for every value of α, the size of the ventricular myocardium within the scope of the unipolar lead was larger than for bipolar leads, thus confirming that the scope is wider for unipolar than for bipolar leads. When comparing true bipolar with integrated bipolar leads, we found that the size of the ventricular myocardium within the scope was smaller for true bipolar than for integrated bipolar leads.

The distribution of the ventricular myocardial mass within the scope of each lead is informative about the anatomical origin of the EGM. Figure 3 shows the estimated scope for every lead for $\alpha = 0.1$. As previously remarked, the unipolar lead showed a wider scope than bipolar leads, and the integrated bipolar lead a wider scope than the true bipolar. Furthermore, the ventricular myocardial mass within the scope of the integrated bipolar lead was found to extend along the septum and anteriorly, while for the true bipolar it was distributed locally close to the lead. Such distribution follows the geometry and location of the electrodes constituting the lead.

4. Discussion and conclusions

Differences in the sensing performance of true and integrated bipolar leads have been reported in the literature [4] [5] [6] [13]. The cause of this discrepancy has not been clearly elucidated. In redetection, for example, it has been postulated that the more likely explanation is myocardial stunning occurring with an integrated bipolar configuration [5]. On the other hand, some authors concentrate on the measurement properties of the lead system, and argue that the quality of the signals recorded by true and integrated bipolar configurations is different [4] [6] [13].

In this paper we maintain that EGM features can be explained by estimating the extent of myocardium within the scope of the lead. We have investigated differences in the scope of true and integrated bipolar leads by means of bioelectric signal modeling and numerical methods. Our results indicate that true bipolar leads have a narrower scope than integrated bipolar leads. Furthermore, we are able to identify the extent of myocardium within the scope of each lead. We have found that the extent of myocardium within the scope of the integrated bipolar lead distributes along the septum and anteriorly, while in the case of true bipolar, it distributes locally around the electrode site. These

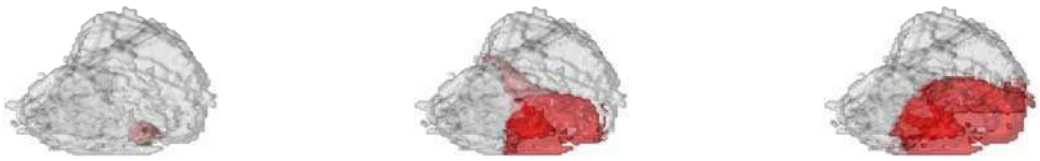

(a) (b) (c)

Figure 3. In red, ventricular myocardial mass within the scope of implemented true bipolar (a), integrated bipolar (b) and unipolar (c) leads.

discrepancies could explain differences in EGM features, such as complex duration, amplitude or slew-rate, and could help to elucidate the anatomical origin of the EGM. The generality of the results of this study depends on the ability of the model to describe the dynamics of cardiac signals and the accuracy of the description of the anatomical model. In the future we will implement more sophisticated thorax and lead models, and simulate cardiac current sources based on other formalisms and stimulation protocols. Furthermore, we will extend this procedure to study other factors, such as lead positioning, type of heart disease and underlying cardiac dynamics.

Acknowledgements

This work has been partially supported by research grant from Guidant Spain, and from Research Project TEC2007-68096-C02/TCM from Spanish Ministerio de Educación y Ciencia. JRC is supported by grant 01-836-04 from Consejería de Educación de la Comunidad de Madrid.

References

[1] Jenkins JM, Caswell SA. Detection algorithms in implantable cardioverter defibrillators. Proc of the IEEE 1996; 84:428–445.

[2] Gradaus R, Breithardt G, Bocker D. ICD leads: design and chronic dysfunctions. Pacing Clin Electrophysiol 2003; 26:649–657.

[3] DeCaprio V, Hurzeler P, Furman S. A comparison of unipolar and bipolar electrograms for cardiac pacemaker sensing. Circulation 1977;56:750–755.

[4] Menz V, Schwartzman D, Drachman D, Michelle JJ, Dillon SM. Recording of pacing stimulus artifacts by endovascular defibrillation lead systems: Comparison of true and integrated bipolar circuits. J Interv Card Electrophysiol 1998; 2:269–272.

[5] Cooklin M, Tummala R, Peters R, Shorofsky S, Gold M. Comparison of bipolar and integrated sensing for redetection of ventricular fibrillation. Am Heart J 1999;138:133–136.

[6] Frain B, Ellison K, Michaud G, Koo C, Buxton A, Kirk M. True bipolar defibrillator leads have increased sensing latency and threshold compared with the integrated bipolar configuration. J Cardiovasc Electrophysiol 2007;18:192–195.

[7] McFee R, Johnston FD. Electrocardiographic leads. I: Introduction. Circulation 1953;8:554–568.

[8] Arzbaecher RC, Jenkins JM, Collins S.and Berbari E. Atrial electrical activity: The view from the esophagus. In Frontiers of Engineering in Health Care, IEEE/EMBS Conference. IEEE Press, 1979; 314–318.

[9] Malmivuo J, Plonsey R. Bioelectromagnetism: Principles and applications of Bioelectric and Biomagnetic Fields. Oxford University Press, NY, 1995.

[10] Kauppinen P, Hyttinen J, Heinonen T, Malmivuo J. Detailed model of the thorax as a volume conductor based on the visible human man data. J Med Eng Technol 1998;22:126–133.

[11] Alonso Atienza F, Requena Carrión J, García Alberola A, Rojo Álvarez JL, Sánchez Muñoz JJ, Martínez Sánchez J, Valdés Chávarri M. A probabilistic model of cardiac electrical activity based on a cellular automata system. Rev Esp Cardiol 2005;58:41–47.

[12] Requena-Carrión J, Väisänen J, Alonso-Atienza F, Rojo-Álvarez JL, Hyttinen J, García-Alberola A. Estimation of the scope of transvenous lead systems in implantable cardioverter defibrillators. In IEEE Proc. Annu. Int. Conf. IEEE EMBS. IEEE Press, 2007; accepted.

[13] Goldberger J, Horvath G, Donovan D, Johnson D, Challapalli R, Kadish A. Detection of ventricular fibrillation by transvenous defibrillating leads: integrated versus dedicated bipolar sensing. J Cardiovasc Electrophysiol 1998; 9:677–688.

Address for correspondence:

José Luis Rojo Álvarez
Departamento de Teoría de la Señal y Comunicaciones B.004
Universidad Rey Juan Carlos
Camino del Molino s/n, 28943, Fuenlabrada, Madrid, Spain
E-mail to: joseluis.rojo@urjc.es